Optical Engineering 48(4), 044001 (April 2009)

New image multiplexing scheme for compensating lens mismatch and viewing zone shifts in three-dimensional lenticular displays

Yun-Gu Lee[*]
Jong Beom Ra, MEMBER SPIE
Korea Advanced Institute of Science and Technology (KAIST)
School of EECS
371-1 Guseongdong
Yuseonggu, Daejeon 305-701
South Korea
E-mail: jbra@ee.kaist.ac.kr

Abstract. A lenticular system provides optimal display quality when a homogeneous lenticular sheet is precisely aligned on LCD subpixels and when a viewer is located within a predetermined viewing zone. In practice, however, many lenticular systems suffer from image distortion due to misalignment or inhomogeneity of the lenticular sheet. To alleviate such distortion, we propose a new multiplexing algorithm. The proposed algorithm first obtains the geometric relationship between LCD subpixels and lenticules by using various pattern images. Then, it generates a mapping matrix between LCD subpixels and multiple-view images based on the obtained relationship. While the proposed scheme is quite simple, it effectively compensates any misalignment or inhomogeneity of the lenticular sheet, and it significantly improves 3-D image quality. In addition, by simply adjusting the mapping parameters, the algorithm can change the predetermined viewing zone to include a viewer's actual position. Experimental results demonstrate that the proposed compensation scheme successfully works in a real 3-D lenticular display system. [DOI: 10.1117/1.3116705]

Subject terms: 3-D display; multiview images; lenticular system; autostereoscopic display; lenticular misalignment; image distortion correction.

Paper 080807R received Oct. 12, 2008; revised manuscript received Feb. 2, 2009; accepted for publication Feb. 10, 2009; published online Apr. 20, 2009. This paper is a revision of a paper presented at the SPIE Conference on Stereoscopic Displays and Virtual Reality Systems XIII, January 2006, San Jose, California. The paper presented there appears (unrefereed) in SPIE Proceedings Vol. 6055.

1 Introduction

In order to visualize 3-D images, various display technologies have been developed, such as anaglyph, volumetric display, lenticular display, parallax barrier display, and integral photography.[1–7] Among these technologies, lenticular display technology is quite popular because it is easily implemented, provides high brightness, and generates multiple views.[3,8]

In a lenticular display system, the LCD pixel array is located at the focal plane of the lenticular sheet, which is a cylinder-shaped lens array. Since the lenticular sheet refracts the light from the LCD pixel array, the images observed through the sheet depend on the viewer's eye position. Thus, images viewed from the left and right eyes differ, so that the viewer may perceive depth information or the system may generate stereoscopic information.[9]

For an N-view lenticular display, a multiview image is prepared by multiplexing N different view images.[10–14] Then, the multiview image is allocated to LCD pixels. Thereby, the lenticular display provides N different views, depending on a viewer's eye position. However, the resolution of an observed view is inversely proportional to N. If the display provides multiple-view images by sacrificing the horizontal resolution only, then the horizontal and vertical resolutions of a 3-D image are unbalanced. Hence, slanted lenticular display systems were introduced to distribute the resolution degradation into both the horizontal and vertical directions.[15]

Slight misalignment between a lenticular sheet and the LCD pixel array causes considerable 3-D image distortion. Hence, a very tedious and difficult alignment procedure is usually required in manufacturing a lenticular display system. However, this alignment procedure is much more difficult for a slanted lenticular system. In order to relax the requirement of alignment accuracy, we proposed the first software approach by suggesting a novel multiview multiplexing method for lenticular display.[16] The method first estimates alignment errors by using a single pattern image. Then, based on the estimated errors, it modifies the multiview image to alleviate the image distortion. Though the proposal suggested a software approach for compensating against distortion and for relocating a viewing position, it is inadequate for real-time applications, due to its complexity in generating a multiview image. Moreover, it cannot compensate any nonlinear distortion caused by an inhomogeneous lenticular sheet. To reduce artifacts in a 3-D image, a method of precompensation by characterizing the light transport function of a display can be considered.[17] However, this method needs an iteration procedure for compen-

[*]Currently at Digital Media R&D Center, Samsung Electronics Company, Ltd., Suwon, Gyeonggido 443-742, South Korea.

0091-3286/2009/$25.00

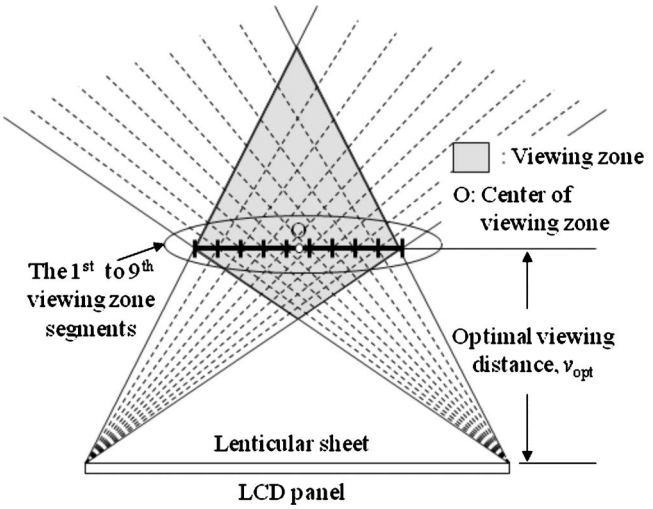

Fig. 1 A nine-view lenticular system with nine viewing zone segments.

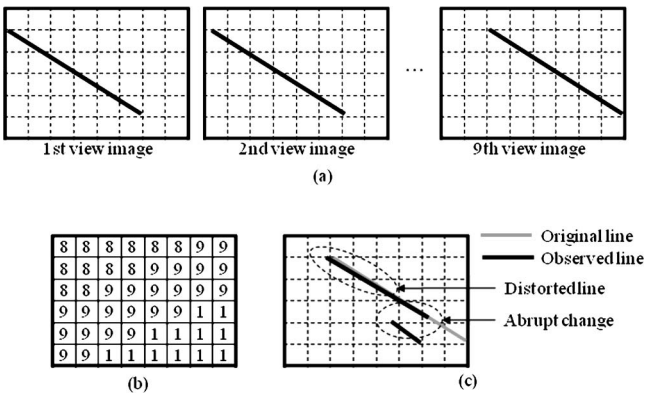

Fig. 2 An example of 3-D image distortion: (a) original view images; (b) view indices at subpixels in an image observed at the ninth viewing zone segment; and (c) the corresponding distorted image. Ideally, all view indices in (b) are to be 9.

sating each image. Hence, it requires a large amount of computation, which is inappropriate for video display.

In this paper, we propose a new multiview multiplexing algorithm. Since the algorithm generates a mapping matrix directly, without calculating misalignment errors between LCD subpixels and a lenticular sheet, it is fairly simple and can compensate any inhomogeneity of the lenticular sheet.

The remainder of this paper is organized as follows. Section 2 describes several problems of lenticular display technology in detail. Section 3 presents the proposed algorithm and shows how it can solve the problems described in Sec. 2 by properly generating a multiview image. Section 4 provides our experimental results. Finally, our conclusions are given in Sec. 5.

2 3-D Image Distortion

Figure 1 demonstrates a nine-view lenticular system having nine viewing zone segments. A viewer's eye located at the k'th viewing zone segment ideally observes only the k'th view image. Thereby, the system provides 3-D images with optimal quality to a viewer located within the limited diamond-shaped viewing zone, as shown in Fig. 1.[18] Note here that the viewing zone is fixed, once the design parameters of the lenticular sheet are determined. If a viewer's eye is located outside the viewing zone,[18] the viewer may not see the correct 3-D image, and an observed image will be distorted. This is considered an intrinsic problem of lenticular display technology.

Furthermore, the lenticular display technology has extrinsic problems caused by the misalignment or inhomogeneity of a lenticular sheet, which can be incurred in the manufacturing process. These extrinsic problems cause unwanted view index shifts in subpixels of the panel and thereby produce image distortions. In order to provide a proper 3-D image, the lenticular sheet should be precisely aligned with the LCD subpixels. Typically, a mapping matrix between a multiview image and the original view images is derived under the assumption of precise alignment between the lenticular sheet and the LCD subpixels.[15] However, if a rotational alignment error exists, then the lenticular pitch along the horizontal direction differs from the original pitch. Accordingly, a multiview image, which is obtained by multiplexing N view images on the basis of the original mapping matrix, will produce distorted 3-D images. Although the amount of error is very small, it noticeably affects the image quality, because the error is accumulated along the horizontal and vertical directions.[16] Note here that the alignment error becomes more considerable when a slanted lenticular sheet is used to remedy the imbalance between the horizontal and vertical resolutions.

A separate problem arises if the lenticular sheet is inhomogeneous. Even a small amount of inhomogeneity can easily cause local lenticule shifts corresponding to several pitches in the panel, which can produce noticeable artifacts. Note here that the pitch error due to the inhomogeneity varies with the geometric location on an LCD panel, while the pitch error due to rotational misalignment is consistent over an entire LCD panel.

An example given in Fig. 2 demonstrates the 3-D image distortion due to the extrinsic and intrinsic problems. Ideally, all the subpixels in an image observed from the ninth viewing zone segment should have the same view index of 9. However, due to the mentioned problems, the subpixels also have view indices different from 9, as in Fig. 2(b). Since errors due to mismatch between LCD subpixels and lenticules are accumulated along the horizontal and vertical directions, the view index increases or decreases along those directions. In addition, the lenticular inhomogeneity causes irregular changes of the view index. Therefore, when a viewer watches the display, a distorted line is observed instead of the desired straight line [see Fig. 2(c)]. Note here that an abrupt change occurs when the view index changes from 9 to 1.

3 3-D Image Multiplexing Method

In this section, we propose a multiplexing algorithm for distortionless 3-D image display in a lenticular system. Although the presented algorithm considers only a nine-view lenticular display system, it can be extended easily to a general N-view system.

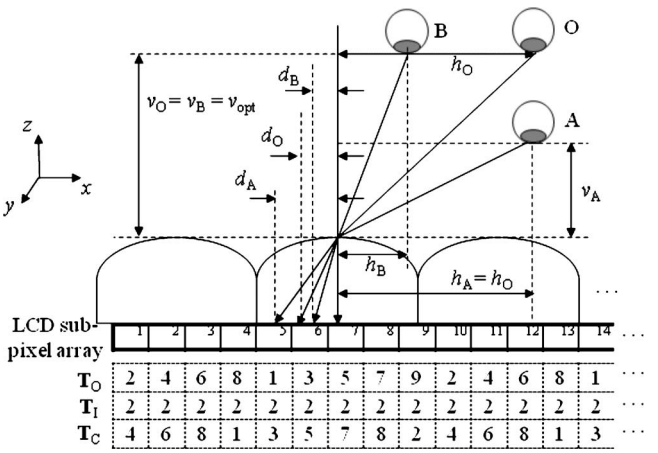

Fig. 3 Changes of a ray path according to the viewer's eye position (or due to an intrinsic problem), and its compensation.

3.1 *Mapping Matrix*

If the intrinsic and extrinsic problems mentioned in Sec. 2 are present, then an observed image includes subpixels sampled from incorrect view images. To compensate for these problems, we attempt to modify the original mapping matrix between LCD subpixels and multiple-view images, $\mathbf{T}_O$, so that a viewer can observe subpixels corresponding to the correct view image. We accomplish this modification by introducing a compensated mapping matrix. This matrix $\mathbf{T}_C$, which is modified from the original mapping matrix $\mathbf{T}_O$, can be written as

$$\mathbf{T}_C = \mathbf{T}_O + \mathbf{T}_E + \mathbf{T}_I. \tag{1}$$

Here, $\mathbf{T}_I$ and $\mathbf{T}_E$ are introduced to compensate for intrinsic and extrinsic problems, respectively. All the matrices have a common size of $L \times 3M$, where L and M denote the vertical and horizontal resolutions of the LCD panel, and their elements have values modulo N. Hence, the (n,m)th elements in the matrices $\mathbf{T}_O$ and $\mathbf{T}_C$ represent the original and compensated view indices of the (n,m)th subpixel on the LCD panel, respectively. Meanwhile, the (n,m)th elements in matrices $\mathbf{T}_I$ and $\mathbf{T}_E$ represent compensation parameters of the view index of the corresponding subpixel. Note that $\mathbf{T}_E$ is invariant for a given 3-D lenticular display system, while $\mathbf{T}_I$ varies according to a viewer's eye position. In the following subsections, we explain how to determine $\mathbf{T}_I$ and $\mathbf{T}_E$ properly. Note that all the values in the matrix are considered as floating-point numbers. Thus, if the view index of a subpixel in $\mathbf{T}_C$ is 3.5, it means that the light emitted from the center of a subpixel on the LCD panel arrives at the middle of the 3rd and 4th viewing zone segments at the optimal viewing distance.

3.2 *Determination of* $\mathbf{T}_I$

To move the viewing zone to a certain position by modifying the mapping matrix, the displacement d between subpixel positions observed in the original viewing zone and those observed in the new viewing zone should be known for every lenticule. In Fig. 3, position O denotes the center of the original viewing zone, or the fifth viewing zone segment, and a viewer wants to move that center along the z axis to position A. If a viewer sees the second lenticule from the left in the figure, subpixels 6 and 5 are observed at positions O and A, respectively, and the displacement d becomes $d_O - d_A$. Here, d_O (or d_A) is easily calculated from Snell's law[19] as

$$d_O = f\frac{h_O}{[n_r^2(v_O^2 + h_O^2) - h_O^2]^{3/2}}, \tag{2}$$

where f is the focal length of the lenticular lenses and n_r is the refractive index of the lenticular sheet. Additionally, h_O and v_O denote the horizontal and vertical displacements from O to the center of the observed lenticule, respectively.

The displacement is interpreted as a shift of view index in the mapping matrix in order to move the center of the original viewing zone. The subpixel location observed from position A is shifted to the left by the width of one subpixel from the position observed from position O. In order to compensate this mismatch, the mapping matrix should be modified by considering this value. Since the view-index difference between successive subpixels in $\mathbf{T}_O$ is 2 for a nine-view slanted lenticular system,[15] the value at the corresponding subpixel in $\mathbf{T}_I$ is set to 2 as in Fig. 3. In general, the value of each subpixel in $\mathbf{T}_I$ is predicted by using the displacement $d(m,n)$, namely,

$$\mathbf{T}_I(m,n) \equiv -\frac{2d(m,n)}{w_{sp}} \pmod 9, \tag{3}$$

where w_{sp} is the width of a subpixel. Similarly, we can also move a viewing zone along the x axis. To move the center of the viewing zone from position O to B, the corresponding displacement becomes $d_O - d_B$, and matrix $\mathbf{T}_I$ can be obtained by using Eq. (3). Therefore, if a system can track and detect a viewer's eye position, the proposed scheme can provide a compensation matrix $\mathbf{T}_I$, so that it can provide the best 3-D image even for an eye located outside the original viewing zone.

In practice, it is not easy to determine an exact h_O, h_A, or h_B, due to the misalignment and inhomogeneity of the lenticular sheet. This makes it difficult to obtain an accurate d_O, d_B, or d_B. However, since the degree of inaccuracy of h_O, h_A, or h_B caused by the misalignment or inhomogeneity of the lenticular sheet is less than a lenticular pitch and is much less than the values of h_O, h_A, or h_B and v_O, v_A, or v_B, its inaccuracy hardly affects the accuracy of the displacement d_O (or d_A). Therefore, we can ignore the extrinsic problems of misalignment and inhomogeneity in calculating the displacement due to the intrinsic problem.

Note here that we do not need to calculate displacements at all the subpixels on the LCD panel. Calculating displacement values only for a small portion of subpixels, we can estimate the remaining displacement values via interpolation. This is because the difference of h_O between neighboring subpixels is much smaller than the value of v_O; therefore, the displacement increases or decreases slowly along the horizontal direction. In addition, displacement values can be considered invariant along the vertical direction even for a slanted lenticular sheet, because the geometrical slant of lenticules hardly affects displacement values. Hence, the calculation of displacement values in only one row is enough to obtain all the values in $\mathbf{T}_I$.

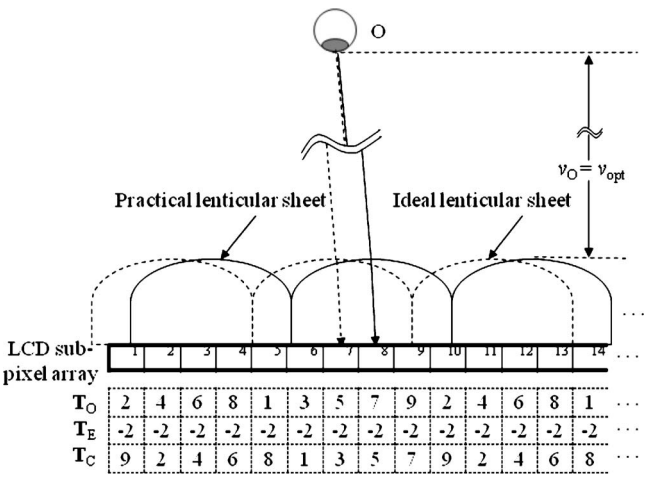

Fig. 4 Change of a ray path due to extrinsic problems and its compensation.

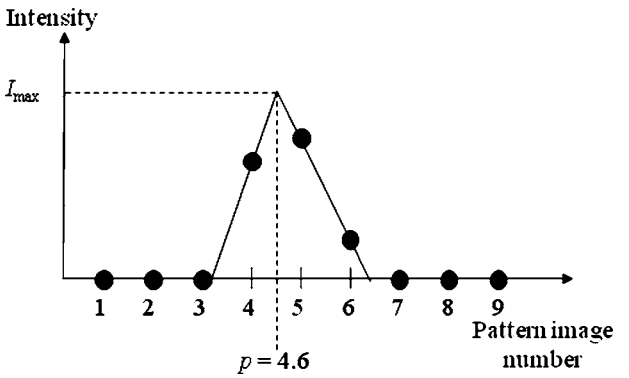

Fig. 5 Intensity peak detection at a subpixel in a set of images that are observed from nine pattern images.

3.3 *Determination of* $\mathbf{T}_E$

In our previous work, we assumed that a lenticular sheet is homogeneous;[16] accordingly, only the misalignment problem of the lenticular sheet was considered. In an inhomogeneous lenticular sheet, however, the lenticular pitch varies with the position. This causes an additional mismatch problem between LCD subpixels and a lenticular sheet. Thus, the error of lenticular pitch should be described on the basis of the two extrinsic problems coming from misalignment and inhomogeneity of the lenticular sheet. In this subsection, we introduce a matrix $\mathbf{T}_E$ used to compensate the mismatch caused by those two problems.

Because the two aforementioned extrinsic problems generate a lenticular pitch error, they change only a geometric relationship between LCD subpixels and the lenticular sheet. Figure 4 demonstrates both the ray-path change caused by the extrinsic problems and the compensation scheme by introducing $\mathbf{T}_E$. In the figure, a viewer's eye located at the fifth viewing zone segment at the optimal viewing distance sees the incorrect subpixel 8 that is sampled from the seventh view image, instead of the correct subpixel 7. To compensate this error and provide a proper 3-D image, the element value of $\mathbf{T}_E$ at the subpixel should be assigned −2. Then, without considering $\mathbf{T}_I$ for the aforementioned intrinsic problem of Eq. (1), the value in the compensated mapping matrix $\mathbf{T}_C$ becomes 5. From this example, we can infer that $\mathbf{T}_E$ can be easily determined if the practical geometric relationship between LCD subpixels and the lenticular sheet is known.

To detect the actual geometric relationship, which has changed from an ideal one due to the extrinsic problems, we propose to use nine multiview pattern images for a nine-view system. We generate the i'th multiview pattern image by setting the i'th view image to white and the others to black and then multiplexing them according to the original mapping matrix. In order to avoid image distortion due to the intrinsic problem, we observe each pattern image at the central (fifth) viewing-zone segment. If there are no extrinsic problems, the fifth image has the maximum intensity among the nine pattern images observed from the fifth viewing-zone segment. In this case, all the elements in $\mathbf{T}_E$ have zero values. However, if extrinsic problems exist, then intensities of the observed nine pattern images continuously vary with the location as well as the pattern image number. As an example, Fig. 5 shows intensity values, which are observed at point (m,n) and graphed according to pattern images. In the figure, we approximate the curve for peak detection with a piecewise linear function for simplicity. Since the peak value is detected at p, $p-5$ can be considered a shift due to extrinsic problems. Hence, the (m,n)th element of $\mathbf{T}_E$ should be set to $5-p$. Note here that p is a floating-point number.

3.4 *Practical Issues in Determining* $\mathbf{T}_C$

In determining $\mathbf{T}_I$ and $\mathbf{T}_E$, we assumed that the optimal viewing distance or position O in the viewing zone is known. Sometimes, however, we may not know position O for a given system, but still want to compensate $\mathbf{T}_O$ for viewing distortion-free 3-D images at a certain viewing zone corresponding to position Q. This practical problem can be solved by observing nine pattern images as described in Sec. 3.3. Since position O is unknown, however, pattern images can be observed at position Q, and the compensation parameter matrix becomes $\mathbf{T}_E(\mathrm{Q})$ rather than $\mathbf{T}_E$ [or $\mathbf{T}_E(\mathrm{O})$], which can be decomposed into

$$\mathbf{T}_E(\mathrm{Q}) = \mathbf{T}_E + \mathbf{T}_I(\mathrm{Q}). \tag{4}$$

Here, $\mathbf{T}_I(\mathrm{Q})$ denotes an intrinsic parameter matrix at position Q. Note here that, since $\mathbf{T}_E(\mathrm{Q})$ includes both $\mathbf{T}_E$ and $\mathbf{T}_I$, $\mathbf{T}_E(\mathrm{Q})$ itself can be used to obtain the compensated mapping matrix at position Q, or $\mathbf{T}_C(\mathrm{Q})$ $[=\mathbf{T}_O+\mathbf{T}_E(\mathrm{Q})]$. If point O is known, $\mathbf{T}_E$ and $\mathbf{T}_I(\mathrm{Q})$ can be separately obtained by using $\mathbf{T}_E(\mathrm{Q})$, since $\mathbf{T}_I(\mathrm{Q})$ can be calculated by Eq. (3).

Now we consider an additional practical problem of moving the viewing zone to an arbitrary point P other than a single fixed position Q where nine pattern images have been observed. In order to move the viewing zone to P while compensating for intrinsic and extrinsic problems, we should calculate $\mathbf{T}_C(\mathrm{P})$, which is represented as

$$\mathbf{T}_C(\mathrm{P}) = \mathbf{T}_O + \mathbf{T}_E + \mathbf{T}_I(\mathrm{P}). \tag{5}$$

Since $\mathbf{T}_E$ cannot be acquired, we may use $\mathbf{T}_E(\mathrm{Q})$ instead. By using Eq. (4), Eq. (5) can be rewritten as

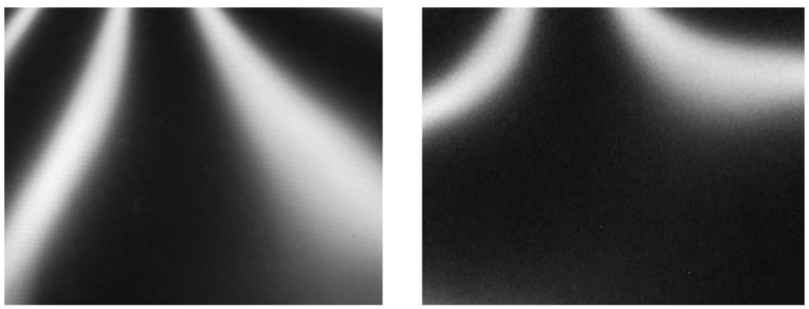

Fig. 6 Pictures of a pattern image, which were taken from the fifth viewing zone at the distances of (a) 400 mm and (b) 1600 mm.

$$\mathbf{T}_C(P) = \mathbf{T}_O + \mathbf{T}_E(Q) - \mathbf{T}_I(Q) + \mathbf{T}_I(P). \quad (6)$$

While $\mathbf{T}_O$ and $\mathbf{T}_E(Q)$ are known, individual values for $\mathbf{T}_I(P)$ and $\mathbf{T}_I(Q)$ cannot be calculated, since position O is unknown. However, the difference, $\mathbf{T}_I(Q) - \mathbf{T}_I(P)$, can still be obtained by calculating the displacement between subpixel locations observed at positions P and Q and applying it to Eq. (3). Thereby, the final compensation matrix $\mathbf{T}_C(P)$ can be obtained simply from the pattern image measurement at Q even without knowing the optimal viewing distance of the system.

4 Experimental Results

To verify the proposed algorithm, we prepared a lenticular display system by attaching a lenticular sheet to an ordinary LCD display and performed experiments with a synthetic 3-D image and an actual 3-D image. The resolution of the LCD panel was 1280×1024, and its dot pitch was 0.264 mm.

Figure 6 represents an example of pictures observed from the fifth pattern image. The pictures were taken by using a digital camera at distances of 400 and 1600 mm, respectively. We can easily notice that the intensity variation in the observed pattern images is not regular or symmetric. Accordingly, we can infer that the lenticular sheet is not homogeneous. In addition, the two observed pictures from the same pattern are different, depending on the distance from the LCD to a viewer. This is because the distortion in an observed 3-D image varies depending on the viewing distance due to the aforementioned intrinsic problem. For example, let us assume that a viewing zone is selected at a distance of 400 mm. Then, by using the nine pattern images including the one shown in Fig. 6(a), $\mathbf{T}_E(Q)$ can be obtained to compensate for 3-D image distortions.

Figure 7 demonstrates the 3-D display performance of the proposed algorithm for a synthetic 3-D image. In this experiment, the pictures shown in Fig. 7(a) and 7(c) were taken from a distance of 400 mm, while those in Fig. 7(b) and 7(d) were taken from a distance of 1600 mm, which represents the changed optimal viewing distance. While

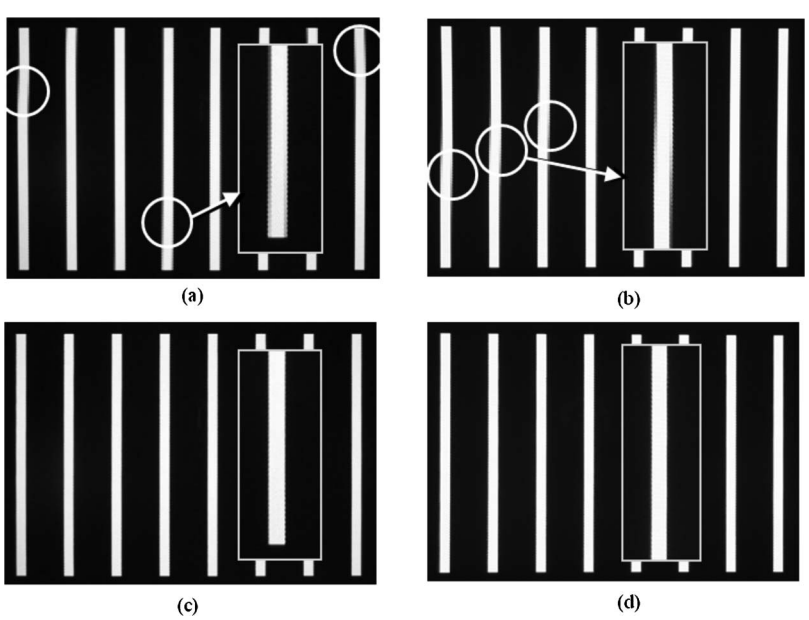

Fig. 7 Pictures of synthesized 3-D images taken from the fifth viewing zone segment with distances of (a), (c) 400 mm and (b), (d) 1600 mm. The synthesized image consists of eight vertically allocated parallel rods. (a), (b) Results without compensation; (c), (d) results with compensation.

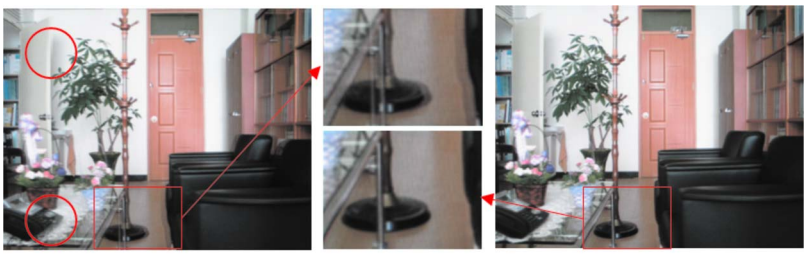

(a) (b)

Fig. 8 Pictures of an actual 3-D image taken from the fifth viewing zone at the distance of 1600 mm: (a) result without compensation; (b) result with compensation.

Fig. 7(a) and 7(b) represent the 3-D image obtained by multiplexing nine view images with the original mapping matrix, Fig. 7(c) and 7(d) represent the 3-D image obtained by using the proposed mapping matrix to compensate intrinsic and extrinsic distortion. The 3-D image in Fig. 7(a) and 7(b) includes unwanted distortions that vary with the camera position. In contrast, the proposed algorithm provides well-improved 3-D images regardless of the camera position. Here, we use two different $\mathbf{T}_I$'s to change the optimal viewing distance to 400 and 1600 mm, respectively.

Figure 8 illustrates the performance of the proposed scheme using an actual 3-D image. Pictures were taken from a distance of 1600 mm. Similarly to the preceding experiment, the 3-D image without compensation includes image distortions, which are well examined inside circles in the left picture. In contrast, the proposed algorithm noticeably compensates the image distortion.

Since $\mathbf{T}_E$ compensates the misalignment and inhomogeneity of a lenticular sheet and is uniquely determined for each product, we can set a unique $\mathbf{T}_E$ to each product during the manufacturing process. Through this simple software approach, we can reduce the performance variation among lenticular display systems manufactured with the same design parameters. We can also reduce the manufacturing cost, because the use of a very homogeneous lenticular sheet and an accurate alignment are expensive, especially for a high-resolution display system having a narrow lenticular pitch.

5 Conclusions

In this paper, we have proposed a new multiplexing algorithm to solve problems that are intrinsic and extrinsic to lenticular display system technology. While our previous work required a considerable computational burden, the newly proposed algorithm significantly reduces the computation complexity by introducing a mapping matrix. The scheme includes the original mapping matrix and two additional matrices to compensate for a viewer's position change, alignment errors, and lenticular sheet inhomogeneity. We have proven that the proposed software approach can obtain good-quality 3-D images regardless of systems' imperfections and/or a viewer's position change.

References

1. E. Dubois, "A projection method to generate anaglyph stereo images," in *Proc. IEEE Conf. on Acoustics Speech and Signal Processing*, Vol. **3**, pp. 1661–1664 (2001).
2. B. G. Blundell and A. J. Schwarz, "The classification of volumetric display systems: characteristics and predictability of the image space," *IEEE Trans. Vis. Comput. Graph.* **8**(1), 66–75 (2002).
3. L. Lipton and M. Feldman, "A new autostereoscopic display technology: the SynthaGram™," in *Stereoscopic Displays and Virtual Reality Systems*, *Proc. SPIE* **4660**, 229–235 (2002).
4. I. Sexon, "Parallax barrier display systems," in *IEE Colloq. on Stereoscopic Television*, pp. 5/1–5/5 (1992).
5. F. Okano, H. Hoshino, J. Arai, and I. Yuyama, "Real-time pickup method for a three-dimensional image based on integral photography," *Appl. Opt.* **36**, 1598–1603 (1997).
6. N. A. Dodgson, "Autostereoscopic 3D displays," *IEEE Computer* **38**(8), 31–36 (2005).
7. W. Matusik and H. Pfister, "3D TV: a scalable system for real-time acquisition, transmission, and autostereoscopic display of dynamic scenes," *ACM Trans. Graphics* **23**(3), 814–824 (2004).
8. A. Schmidt and A. Grasnick, "Multi-viewpoint autostereoscopic displays from 4D-Vision," in *Stereoscopic Displays and Virtual Reality Systems*, *Proc. SPIE* **4660**, 212–221 (2002).
9. C. V. Berkel, A. R. Franklin, and J. R. Mansell, "Design and applications of multiview 3D-LCD," in *Proc. SID Euro-Display 96*, pp. 109–112 (1996).
10. J. Konrad and P. Agniel, "Artifact reduction in lenticular multiscopic 3-D displays by means of anti-alias filtering," in *Stereoscopic Displays and Virtual Reality Systems*, *Proc. SPIE* **5006A**, 336–347 (2003).
11. J. Konrad and P. Agniel, "Subsampling models and anti-alias filters for 3-D automultiscopic displays," *IEEE Trans. Image Process.* **15**(1), 128–140 (2006).
12. J. Konrad and P. Agniel, "Non-orthogonal sub-sampling and anti-alias filtering for multiscopic 3-D displays," in *Stereoscopic Displays and Virtual Reality Systems*, *Proc. SPIE* **5291A**, 105–116 (2004).
13. K. Mashitani, G. Hamagishi, M. Higashino, T. Ando, and S. Takemoto, "Step barrier system multi-view glass-less 3-D display," in *Stereoscopic Displays and Virtual Reality Systems*, *Proc. SPIE* **5291**, 265–272 (2004).
14. C. N. Moller and A. R. L. Travis, "Correcting interperspective aliasing in autostereoscopic displays," *IEEE Trans. Vis. Comput. Graph.* **11**(2), 228–236 (2005).
15. C. V. Berkel, "Image preparation for 3D-LCD," in *Stereoscopic Displays and Virtual Reality Systems*, *Proc. SPIE* **3639**, 84–91 (1999).
16. Y. G. Lee and J. B. Ra, "Image distortion correction for lenticular misalignment in 3D lenticular displays," *Opt. Eng.* **45**(1), 017007 1–9 (2006).
17. J. Napoli, S. R. Dey, S. Stutsman, O. S. Cossairt, T. J. Purtell II, S. L. Hill, and G. E. Favalora, "Imaging artifact precompensation for spatially multiplexed 3-D displays," in *SPIE, Stereoscopic Displays and Applications XIX*, *Proc. SPIE* **6803**, 680304 (2008).
18. N. A. Dodgson, "Analysis of the viewing zone of multi-view autostereoscopic displays," in *Stereoscopic Displays and Virtual Reality Systems*, *Proc. SPIE* **4660**, 254–265 (2002).
19. D. Halliday, R. Resnick, and J. Walker, *Fundamentals of Physics*, John Wiley and Sons, New York (2001).

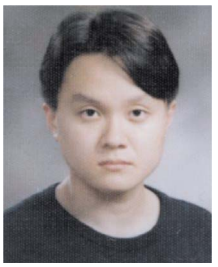

Yun-Gu Lee received his BS, MS, and PhD degrees in electrical engineering and computer science from the Korea Advanced Institute of Science and Technology (KAIST), Daejeon, Korea, in 2000, 2002, and 2006, respectively. He is currently working in the Digital Media R&D Center, Samsung Electronics, Suwon, Korea. His research interests include digital image processing, video signal processing, and 3-D display system.

Jong Beom Ra received his BS degree in electronic engineering from Seoul National University, Seoul, Korea, in 1975, and his MS and PhD degrees in electrical engineering from the Korea Advanced Institute of Science and Technology (KAIST), Daejeon, in 1977 and 1983, respectively. From 1983 to 1987, he was an associate research scientist with Columbia University, New York. Since 1987, he has been a professor in the Department of Electrical Engineering and Computer Science, KAIST, where he currently directs the Image Information Research Center. His research interests are digital image processing, video signal processing, 3-D visualization, 3-D display systems, and medical imaging. He is a member of the SPIE and a senior member of the IEEE.